International Journal of Energy and Environmental Engineering
a SpringerOpen Journal

ORIGINAL RESEARCH Open Access

Analysis and optimization of current collecting systems in PEM fuel cells

Peiwen Li[1*], Jeong-Pill Ki[1,2] and Hong Liu[1]

Abstract

This paper presents analytical and experimental studies on optimization of the gas delivery and current collection system in a proton exchange membrane (PEM) fuel cell for the objective of reducing ohmic loss, thereby achieving higher power density. Specifically, the dimensions of current collection ribs as well as the rib distribution were optimized to get a maximized power density in a fuel cell. In the modeling process, the power output from a fixed area of membrane is calculated through analysis of an electrical circuit simulating the current from electrochemical reaction flowing to the current collectors. Current collectors of two-dimensional ribs and three-dimensional pillars were considered. Analyses found that three-dimensional pillars allow higher power density in a PEM fuel cell. Considering the mass transfer enhancement effect, three-dimensional pillars as current collectors in gas flow field may be a good choice if the fuel cell operates at low current density and there is no liquid water blocking the flow channels. The analyses did not consider the existence of liquid water, meaning the current density is not very high. The study concluded that decreasing the size of both the current collector and its control area yields a significant benefit to a higher power density. A preliminary experimental test in a PEM fuel cell has verified the conclusion of the analytical work.

Keywords: Proton-exchange-membrane fuel cell, Optimization, Current collectors, Analysis

Background

As environmentally friendly power sources, proton exchange membrane (PEM) fuel cells have received increased attention in recent years. Emphasis of research has either been placed on producing high power density with adequate energy conversion efficiency for mobile power source applications or on high energy efficiency with adequate power density for stationary power source applications. One of the big hurdles to the widespread commercialization of fuel cells is due to the high cost and insufficiently high power densities.

One of the important approaches to having high power density in a fuel cell is to reduce the internal losses. The internal losses can always be attributed to the three types of polarizations [1]: activation polarization, concentration polarization, and ohmic polarization. As these polarizations increase, the overpotential can become too large for the fuel cell to produce a high power density with reasonably high energy efficiency [2-4]. The minimization of polarization will largely depend on the mechanism that causes each specific type of polarization. The activation polarization is caused by the slowness of the electrochemical reactions taking place on the surface of the electrodes. Consequently, a proportion of the available ideal voltage is sacrificed in the electrochemical reaction. The concentration polarization is due to mass transfer resistance from bulk flow to the surface of the electrodes when fuel and oxygen are consumed and water is generated. The ohmic polarization is the straightforward resistance to the flow of electrons through the material of the electrodes and the various interconnections as well as the resistance to the flow of protons through the electrolyte.

The reduction of activation polarization is largely related to membrane and catalyst properties. The electrical potential loss due to ohmic and concentration polarization is strongly related to the configurations of the current conduction and collection elements [5,6]. These elements also significantly affect the mass transfer process since the current collectors are ribs or walls that guide the flow of reactant and product species in a fuel

* Correspondence: peiwen@email.arizona.edu
[1]Department of Aerospace and Mechanical Engineering, University of Arizona, Tucson, AZ, 85721, USA
Full list of author information is available at the end of the article

cell [7,8]. The total of ohmic polarization and concentration polarization may take a large proportion in the overall losses of fuel cell if the flow channels are not well designed or if the contact resistances between cell components are large [9,10].

A qualitative description of the control and optimization of ohmic loss is worth reviewing here. On an electrode/electrolyte layer with a fixed area, using small current collectors can expose a larger membrane area to reactant gases, therefore extracting greater current from the electrochemical reaction. However, a smaller current collector has a small contact area to electrodes and also makes the pathway for current conducting along the in-plane direction of electrode layers longer. This increases the ohmic loss. To strike the best balance between the two competing effects, an optimal arrangement of the current collectors on a bipolar plate is needed. This raises issues about optimization of the size of a current collector and the area from which the current due to electrochemical reaction is collected [11,12]. Obviously, the objective of this optimization is to obtain a maximum power density on an electrode/electrolyte membrane in a fixed area.

The minimization of the fuel cell voltage losses due to mass transfer and ohmic resistances will largely depend on the design of gas flow fields and current collecting system on the bipolar plates. The bipolar plates perform functions including the electrical connection between cells, supply of reactant gases, water and heat management, and support for membrane electrode assembly (MEA). Improvement in the design of current collecting and flow delivery system is therefore important to the high efficiency and maximized power density in fuel cells.

Various bipolar plate designs have been tested and evaluated by researchers worldwide in the field of PEM fuel cells [13,14]. The considered factors include the following: properties of materials [15], cost benefit analysis [16], the optimization of flow field [17], etc. The essential objective of these analyses is to achieve a maximum power output at low cost of materials of bipolar plates.

In this study, the analyses for the optimization of a current collection system will consider two different structures of current collectors. The first type is a two-dimensional (2D) rib design which is very common in proton exchange membrane fuel cell (PEMFC) products so far; the second type is a three-dimensional (3D) pillar design. The analysis will find optimal sizes of ribs and pillars in a given area of membrane to meet the objective of maximum power density. The same optimization analysis will be carried further for different sizes of the given area of the membrane. Using these results, optimal sizes and ratios of the current collectors and their control areas will be recommended for fuel cell design.

There are several published papers that present optimization of the flow channels and current collecting ribs using computational fluid dynamics (CFD) methods [6,10,13]. The models and methods used in these papers are CFD-based and inconvenient for a quick design optimization as might be incidentally required. To avoid the heavy-load numerical computations, the current paper presents a model that can be easily implemented. It considered typical flow channel and current collector structures as they possess the common features of current collection processes in PEM fuel cells. The model and results presented are of significance to the practical design of fuel cells when heavy CFD analysis is unavailable.

Methods

Structure of current collectors

The long gas channels and two-dimensional ribs shown in Figure 1 are typical characteristics of a bipolar plate in a fuel cell. From the mass transfer point of view, this flow field design has disadvantages in promoting the mixing of flows. To mitigate this shortcoming, 3D pillars, shown in Figure 2, for current collection and mass transfer enhancement have been proposed [18] for solid oxide fuel cells by one of the current authors. In order to give a comprehensive study of the current collectors, the present physical model will analyze both 2D and 3D current collecting elements in the gas delivery field of PEM fuel cells.

Analytical model

To analyze the current collecting system, it is convenient to consider just one single collector which collects the current of the electrochemical reaction in a controlled area. An electrical circuit will establish the relationship

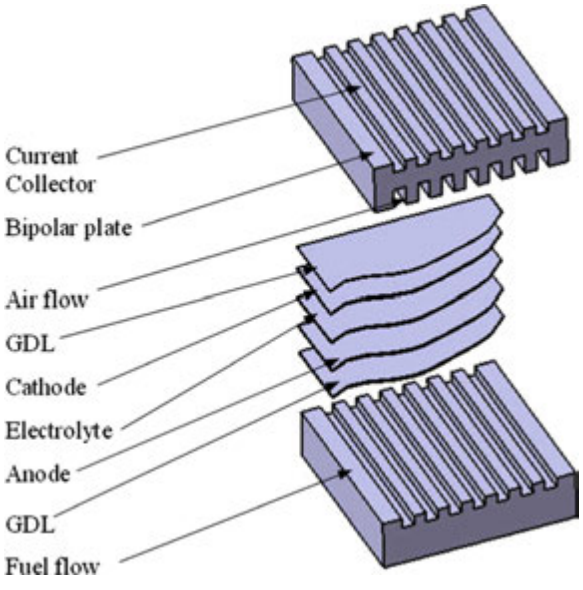

Figure 1 Two-dimensional current collectors on a bipolar plate.

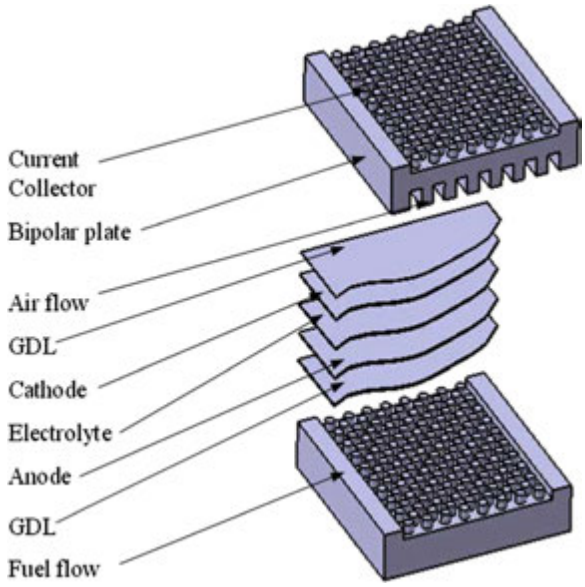

Figure 2 Three-dimensional current collectors on a bipolar plate.

of the relevant parameters to the power density. These parameters include the dimensions of current collectors and control area, the fuel cell operating temperature, and properties of the membrane and electrodes. The effect of current collection area and current collector size on the power density will be discussed in order to find optimal dimensions.

Figures 3 and 4, respectively, show the physical models of a single current collector and the electrical circuits for 2D-type and 3D-type collectors in a PEMFC. Resistances in the anode, cathode, electrolyte, and gas diffusion layers (GDL) are considered. Contact resistances of the gas diffusion layer to electrodes and gas diffusion layer to current collectors are also considered. Tables 1 and 2 give the properties of all components such as thicknesses, resistivities (at 25°C), and contact resistances. In the gas diffusion layer and electrodes, only resistances in the in-plane direction are considered to be significant. For proton conduction in the electrolyte, resistance is in the through-plane direction.

At a given current density for an area (with a width of d_o for 2D case and a diameter of d_o in 3D case) of the MEA layer, the voltage difference between the cathode-side and the anode-side current collectors can be found through analysis of the circuit. Given conditions include the Nernst potentials and the resistances from contact and conduction. The potentials on every node in the circuit can be related using equations from Kirchhoff's laws.

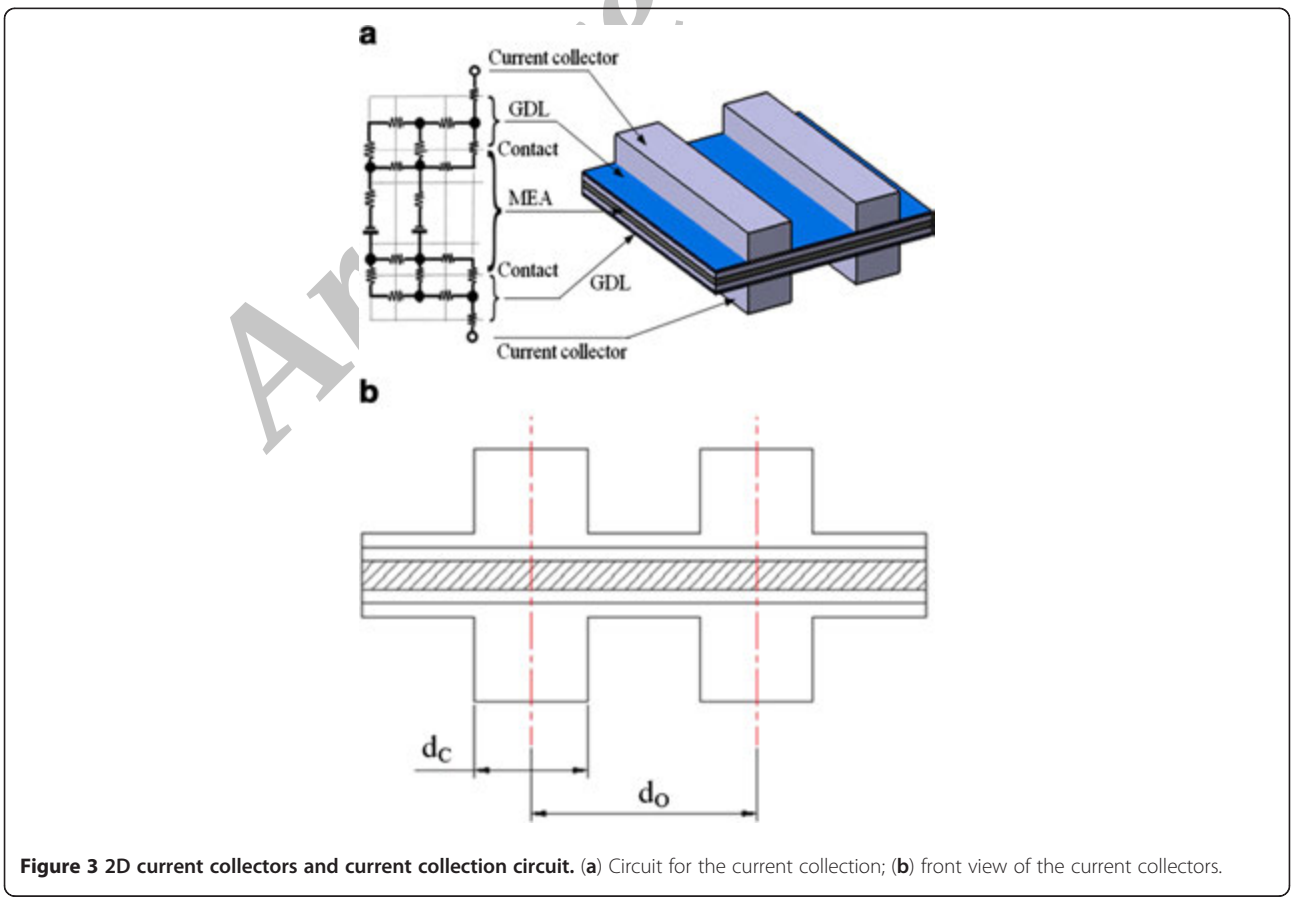

Figure 3 2D current collectors and current collection circuit. (**a**) Circuit for the current collection; (**b**) front view of the current collectors.

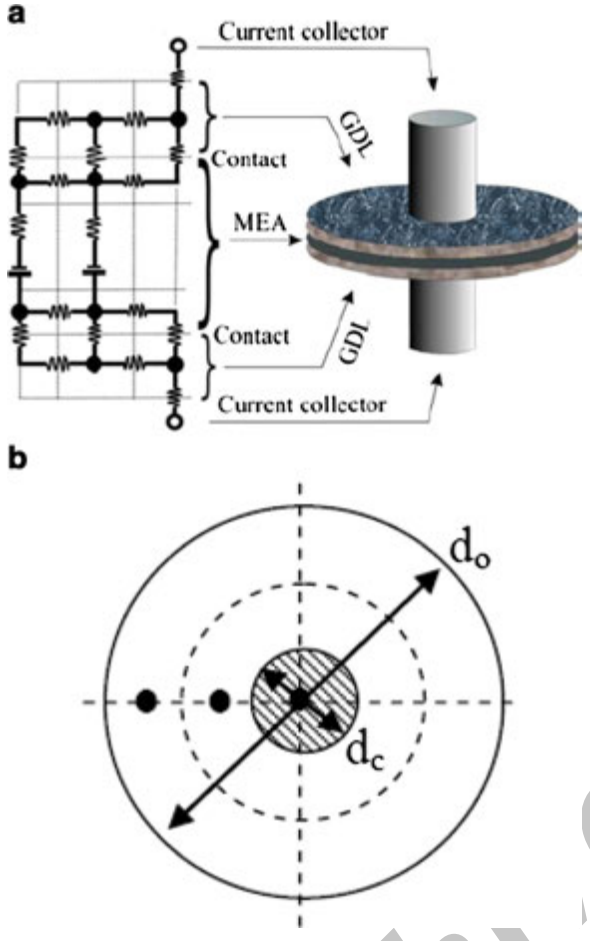

Figure 4 3D current collectors and current collection circuit. (**a**) Circuit for the current collection; (**b**) top view of grid allocation.

Consequently, potentials are available when the equations from all nodes are jointly solved. With potentials known, the power output from the electrode/electrolyte layer of a fixed area is obtained.

The analysis of the current collection may be based on given voltages (at anode-side $V = 0$, and at cathode-side $V = V_{\text{cell}}$). The total current leaving the cathode is calculated once the potentials at all grids in the circuit are obtained [19].

Table 1 Parameters of simulated PEMFC components showing contact resistances

Studied contact resistances(Ω cm^2)		
Anode-GDL	Cathode-GDL	Current collector-GDL
0.001	0.001	0.001
0.005	0.005	0.005
0.010	0.010	0.010
0.015	0.015	0.015

Table 2 Parameters of simulated PEMFC components showing thicknesses and resistivities

	Anode	Cathode	Electrolyte	GDL
Resistivity (Ω cm)	1.8868	1.8868	9.091	0.0127
Thickness (μm)	10	10	100	100

The electromotive forces (emf) in the circuit shown in Figures 3a and 4a are

$$E = E^o - \eta_{\text{conc}} - \eta_{\text{act}}, \tag{1}$$

where the standard state emf, E^o, is based on the low heating value for the electrochemical reaction in a PEM fuel cell; η_{conc} is the concentration polarization. The activation polarization η_{act} is based on equations taken from literature [20]:

$$\eta_{\text{act}} = \frac{RT}{0.5F} \ln\left[\frac{ip^{\text{c}}}{i_{\text{O}_2} p^{\text{c}}_{\text{O}_2}}\right] + \frac{RT}{F} \ln\left[\frac{ip^{\text{a}}}{i_{\text{H}_2} p^{\text{a}}_{\text{H}_2}}\right], \tag{2}$$

where i is the current density; i_{H_2} (1,000 A/m^2 [10]) and i_{O_2} (100 A/m^2 [20]) are the exchange current densities of the anode and cathode sides, respectively; p^{a} is the pressure on the anode side, and p^{c} is that on the cathode side; $p^{\text{a}}_{\text{H}_2}$ and $p^{\text{c}}_{\text{O}_2}$ are the partial pressures of hydrogen on the anode side and oxygen on the cathode side, respectively; T is the temperature of the electrochemical reaction. Table 3 lists several cases identified by the control area of a current collector.

The optimization and fuel cell performance are studied at temperatures of 25°C, 50°C, 60°C, and 75°C. The temperature is used to calculate the ideal electromotive force in Equation 1. Also, the protonic conductivity in the membrane varies depending on the temperature,

$$\sigma(T) = (0.005139\lambda - 0.00326) \exp\left[1,268\left(\frac{1}{303} - \frac{1}{273 + T}\right)\right], \tag{3}$$

where $\lambda > 1$. This parameter is specifically defined as the number of moles of water per number of sulfonic sites in the membrane:

Table 3 The size of control area (d_o)

Number	3D type (mm)	2D type (mm)
a	1.5	1.5
b	1.8	1.8
c	2.0	2.0
d	3.0	3.0
e	4.0	4.0
f	6.0	6.0

Table 4 The values of protonic conductivity and resistivity depending on the operating temperature

Temperature (°C)	Protonic conductivity (1/Ωcm)	Resistivity (Ωcm)
25	0.1100	9.0910
50	0.1529	6.5401
60	0.1720	5.8128
75	0.2027	6.5401

$$\lambda = \frac{\text{number of molecules}}{\text{number of sulfonic sites}}. \quad (4)$$

In this simulation, the water content was considered to be approximately 14 [20], assuming that the membrane is well hydrated. Protonic conductivity was calculated by Equation 3 to consider the effect of temperature. Some values of the protonic conductivity at different temperatures are listed in Table 4.

Results and discussions

The voltage and current density relationships obtained for a fixed area centered by a current collector are presented in the following sections. The concentration polarization is not considered in this optimization analysis. Because of this, the results of the maximum power density obtained in the study will thus be considered as the asymptotic power under the selected operating conditions.

Optimization of the size of 3D current collector/pillar in the center of a fixed control area

This optimization selected an operating temperature of 25°C for analysis. The contact resistance of $R_{cont} = 0.001$ Ω cm^2 between current collectors, gas delivery layers, and electrodes is assumed. Cylindrical current collectors, as shown in Figure 4, are investigated first. The cases of control areas of diameters 2.0, 4.0, and 6.0 mm were considered.

The cell voltages and power densities on a control area centered by a current collector are shown against the current densities in Figure 5. It is clear that current collectors of different sizes will result in different maximum power densities. An optimal current collector diameter is found to be 0.72 mm for the case of a control area with diameter of 2 mm, which can result in a maximum power density of 1.1233 W/cm^2. Results from the cases of control areas of 4.0 mm and 6.0 mm show similar scenarios, although the optimal sizes of current collectors are different in each case.

It is also found that a higher optimized power density is available from a smaller control area. The maximum power density at the optimal current collector size of $d_c = 0.72$ mm in the case of $d_o = 2$ mm is higher than that obtained in the case of $d_c = 2.77$ mm when $d_o = 6$ mm. This feature is observed even when different contact resistances, ranging from $R_{cont} = 0.001$ to $R_{cont} = 0.015$, are applied. These results strongly suggest that densely distributed small-sized 3D-type current collectors in a gas delivery field are preferable. To give a clear

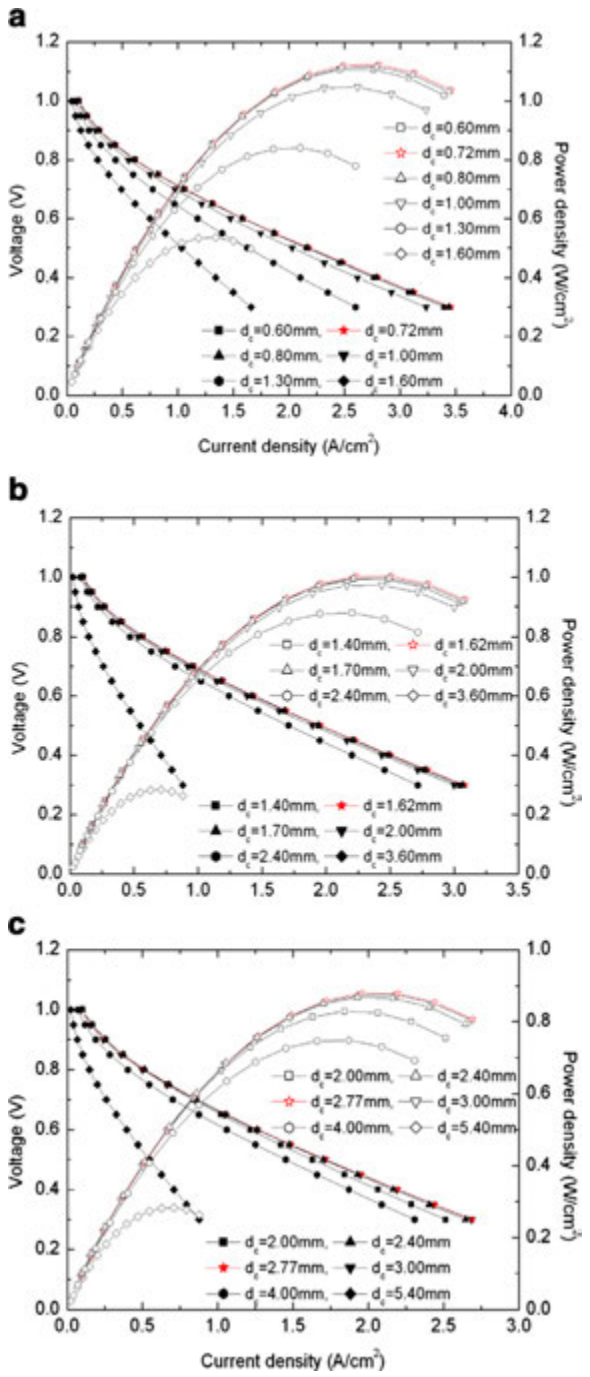

Figure 5 Optimum current collector size in a fixed control area. (**a**) $d_o = 2.0$ mm, (**b**) $d_o = 4.0$ mm, and (**c**) $d_o = 6.0$ mm.

Table 5 The optimum current collector sizes and maximum power density

Contact resistance (Ω cm^2)	Size of control area d_o(mm)	Optimum size of collector d_c(mm)	Maximum power density (W/cm^2)
0.001	1.5	0.53	1.1457
	1.8	0.64	1.1329
	2.0	0.72	1.1233
	3.0	1.14	1.0673
	4.0	1.62	1.0038
	6.0	2.77	0.8797
0.005	1.5	0.70	0.8487
	1.8	0.84	0.8441
	2.0	0.91	0.8396
	3.0	1.44	0.8193
	4.0	1.96	0.7924
	6.0	3.12	0.7300
0.010	1.5	0.78	0.6836
	1.8	0.94	0.6810
	2.0	1.05	0.6791
	3.0	1.59	0.6674
	4.0	2.14	0.6524
	6.0	3.33	0.6153
0.015	1.5	0.83	0.5836
	1.8	0.99	0.5817
	2.0	1.11	0.5803
	3.0	1.67	0.5724
	4.0	2.24	0.5624
	6.0	3.45	0.5370

comparison of the obtained results, Table 5 includes the optimal current collector size and the maximum available power density in different control areas. Figure 6 shows the results given in Table 5.

Firstly, the contact resistance has a significant effect on the maximum available power density. With the decrease of the contact resistance, the maximum output power density increases. The contact resistance is related to many parameters such as clamping force, elastic modulus, thickness of MEA, the pressure of fuel and oxidant, temperature, and humidity [21]. Of these various parameters, the clamping force is relatively important. If the clamping force is unreasonably small, the interfacial contact resistance between the gas diffusion layer and current collector will increase and the maximum power output will decrease [22,23]. The curves of d_o versus d_c in Figure 6 show that ideal current collector sizes exist for the specific contact resistance. This result reminds fuel cell manufacturers that the assembly of PEM fuel cell components should be carefully considered in order

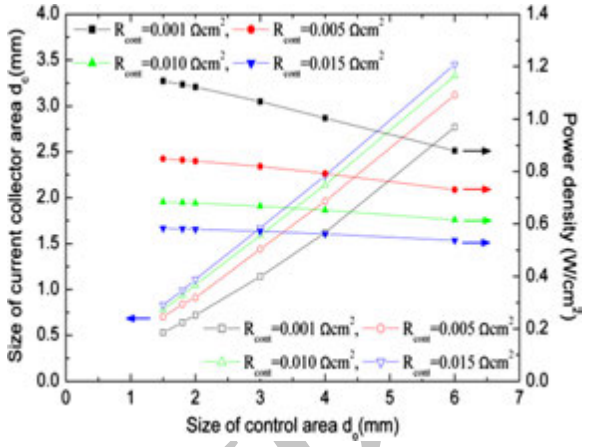

Figure 6 Optimum values of power density and d_o versus d_c at cases with different contact resistances.

to attain the optimal compaction pressure for the appropriate contact resistance. If the contact resistance varies significantly, the effect of optimization of the current collectors may not be maintained.

Optimization of the size of 2D rib current collectors

The two-dimensional current collection ribs, shown in Figure 1, are commonly adopted in commercially available PEM fuel cells. At a contact resistance of R_{cont} = 0.001 Ω cm^2 and electrochemical reaction temperature of 25°C, the optimal current collectors and maximum power densities are obtained for control areas (denoted by d_0) of 1.5, 1.8, 2.0, 3.0, 4.0, and 6.0 mm. As shown in Figure 7, results similar to those from the 3D-type current collectors have been obtained; small control

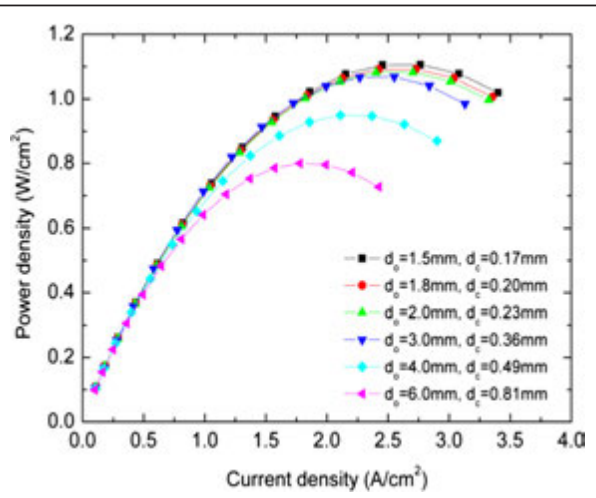

Figure 7 Power density versus current density from optimized current collector at different control areas.

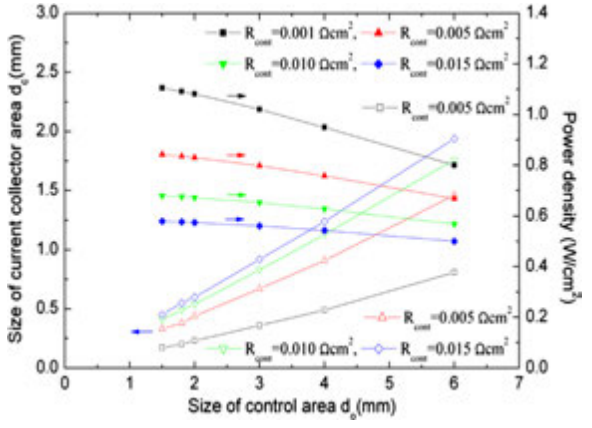

Figure 8 Optimum sizes of 2D current collection ribs and power density for different control areas.

areas and optimized current collectors are advantageous due to the corresponding higher power densities.

A similar investigation for 2D current collection ribs at different contact resistances is also made. Again, for all the cases, the power densities increase when the control area decreases and the current collector width is optimized. Contact resistances significantly affect the maximum output power.

The analytical results of 2D current collecting ribs from Figure 8 are also given in Table 6 for the convenience of comparison between different cases.

Comparison of the optimization result of 3D current collectors and 2D current collectors

It is interesting and of significance to compare the maximum available power densities based on geometrically different types of current collectors. Table 7 shows the maximum power densities obtained from the analysis for 3D cylindrical and 2D rib-type current collectors. The

Table 6 Optimum current collector sizes and maximum power density at different contact resistances for 2D ribs

Contact resistance (Ω cm^2)	Control area size (mm)	Optimum size (mm)	Maximum power density (W/cm^2)
0.001	1.5	0.17	1.1056
	1.8	0.20	1.0917
	2.0	0.23	1.0817
	3.0	0.36	1.0209
	4.0	0.49	0.9495
	6.0	0.81	0.8003
0.005	1.5	0.33	0.8429
	1.8	0.38	0.8357
	2.0	0.44	0.8307
	3.0	0.67	0.7983
	4.0	0.91	0.7583
	6.0	1.46	0.6681
0.010	1.5	0.41	0.6792
	1.8	0.49	0.6750
	2.0	0.54	0.6718
	3.0	0.83	0.6522
	4.0	1.13	0.6273
	6.0	1.76	0.5685
0.015	1.5	0.45	0.5800
	1.8	0.55	0.5769
	2.0	0.60	0.5747
	3.0	0.92	0.5610
	4.0	1.24	0.5434
	6.0	1.94	0.5007

Table 7 Comparison of maximum power density obtained from using 3D-type and 2D-type current collectors

Contact resistance (Ω cm^2)	Size of control area d_o (mm)	Maximum power density for 3D collectors (W/cm^2)	Maximum power density for 2D collectors (W/cm^2)
0.001	1.5	1.1457	1.1056
	1.8	1.1329	1.0917
	2.0	1.1233	1.0817
	3.0	1.0673	1.0209
	4.0	1.0038	0.9495
	6.0	0.8797	0.8003
0.005	1.5	0.8487	0.8429
	1.8	0.8441	0.8357
	2.0	0.8396	0.8307
	3.0	0.8193	0.7983
	4.0	0.7924	0.7583
	6.0	0.7300	0.6681
0.010	1.5	0.6836	0.6792
	1.8	0.6810	0.6750
	2.0	0.6791	0.6718
	3.0	0.6674	0.6522
	4.0	0.6524	0.6273
	6.0	0.6153	0.5685
0.015	1.5	0.5836	0.5800
	1.8	0.5817	0.5769
	2.0	0.5803	0.5747
	3.0	0.5724	0.5610
	4.0	0.5624	0.5434
	6.0	0.5370	0.5007

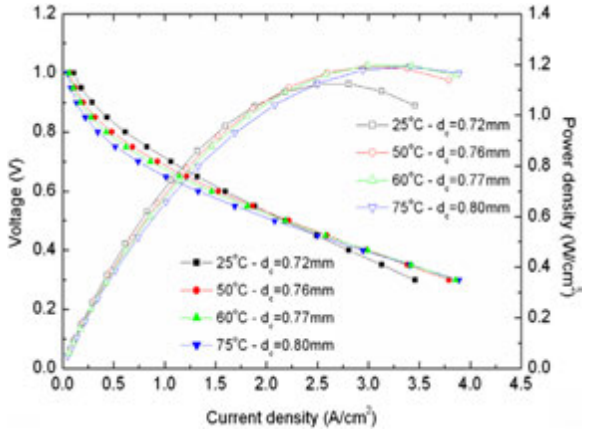

Figure 9 Optimum power density at different temperatures for 3D pillar current collectors (R_{cont} = 0.001 Ω cm^2, d_o = 2.0 mm).

definition for the dimensions of d_o is given in Figures 3 and 4 for 3D and 2D current collectors, respectively. A general trend is identified from this comparison: the maximum power density from using the 3D cylindrical current collector is higher than that from using 2D ribs. This conclusion is drawn without considering the liquid water effect in PEM fuel cells. About 4 % to 7 % of improvement of the maximum power density may be available if 3D cylindrical current collectors are used instead of 2D ribs. Note that for Table 7, the optimum sizes of the current collectors for every case can be found in Tables 5 and 6.

Applicability of optimization effect at different operating temperatures

The fuel cell operating temperatures affect the performance in a complicated manner. Temperature affects the mass transfer polarization since the gas diffusivities are functions of temperature. Temperatures also affect the ideal electromotive force, protonic conductivity of the membrane, and activation polarization. Since the concentration polarization is not considered in the optimization analysis in this work, results regarding the effect of temperature on the maximum available power density are only preliminary studies.

Figure 9 shows the optimized power densities and voltages against current densities for cases of operating temperatures from 25°C to 75°C. The contact resistance is 0.001 Ω cm^2, and the control area size is d_0 = 2.0 mm for a cylindrical current collector. Similarly, Figure 10 indicates the same type of results for 2D rib current collectors. The values for d_c given in Figures 9 and 10 are optimized sizes of current collectors under the different temperatures. Since the increase of temperature will result in an increase of protonic conductivity, higher optimum power density may be available when the operating temperature is high.

Experimental results

In the experimental work by Hental et al. [24], a similar phenomenon as revealed in the present optimization analysis was observed in the development of new materials of current collectors for PEMFCs. They reported that using smaller current collecting ribs and gas channels elicited higher power density in PEM fuel cells. This agrees with the conclusion obtained in the present analysis.

In this study's accompanying experimental work, a test for PEM fuel cells was conducted at room temperatures (25°C) to verify the conclusions from the analytical work. The tested fuel cells have the same membrane, but the current collector size and control area in hydrogen and oxygen flow fields on the bipolar plates are different. One has large-sized 3D current collectors, and the other has

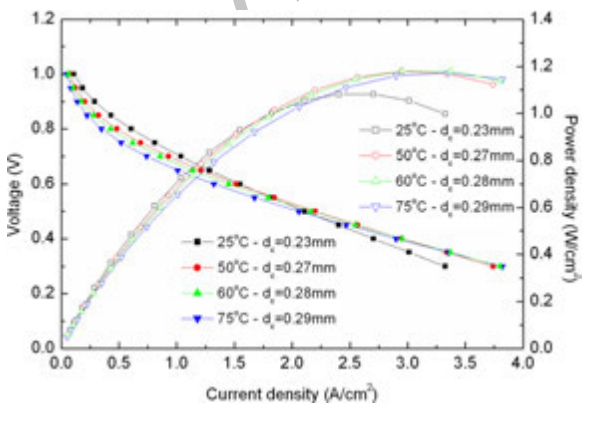

Figure 10 Optimum power density at different temperatures for 2D rib current collectors (R_{cont} = 0.001 Ω cm2, d_o = 2.0 mm).

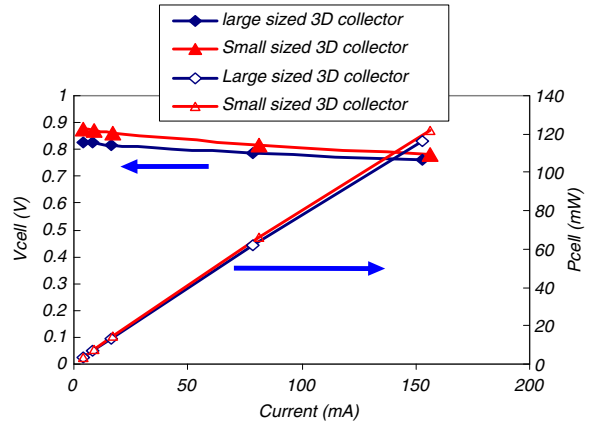

Figure 11 Experimental test for fuel cells at room temperature (25°C). Oxygen was supplied from free convection airflow.

small-sized 3D current collectors. Oxygen with no humidification is provided through natural convective airflow. As shown in Figure 11, a higher voltage output is obtained for small 3D current collectors. A comprehensive experimental test will be carried out in the near future.

Conclusions

Analysis and experimental work was conducted to optimize the flow field and current collectors in PEM fuel cells. From the analysis, the dimensions of current collecting ribs and the rib distribution can be optimized in order to have maximum power density in a fuel cell. The analytical models consider current collectors of two-dimentional ribs and three-dimensional pillars. Upon optimization, using three-dimensional pillars in a flow field can obtain higher power density in a PEM fuel cell. This conclusion is drawn without considering the liquid water effect in PEM fuel cells.

It is also found that higher power densities can be obtained using smaller current collectors with optimized distribution in a flow field. Considering the mass transfer enhancement effect, three-dimensional pillars, as current collectors in gas flow field, are recommended. However, when liquid water exists in a PEMFC, two-dimensional ribs are usually better as the liquid can be excluded with more ease than in the case of three-dimensional pillars. A preliminary, yet not comprehensive, experimental test at low current density without liquid water in PEM fuel cells has found better performance when small sized 3D current collecting pillars and optimal distribution are adopted in a flow field.

Competing interests

The authors declare that they have no competing interests.

Acknowledgment

The support from the Office of Naval Research of the USA and the University of Tennessee SimCenter under the contract #8500011366 is gratefully acknowledged.

Author details

[1]Department of Aerospace and Mechanical Engineering, University of Arizona, Tucson, AZ, 85721, USA. [2]Current address: Department of Mechanical and Aerospace Engineering, University of Texas at Arlington, Arlington, TX, 76019, USA.

Authors' contributions

PL conceived the concept and procedures of the optimization analysis and drafted the manuscript. JK carried out computations and analysis. HL checked equations and analysis, and updated and revised the manuscripts. All authors read and approved the final manuscript.

Authors' information

PL earned his Ph.D. (1995) degree in energy and power engineering area from Xi'an Jiaotong University, China. He is currently an assistant professor in the Department of Aerospace and Mechanical Engineering at the University of Arizona, USA. He has been interested in heat transfer enhancement in industrial processes, turbulence drag reduction, gas turbine cooling technologies, the multi-physics transport phenomena in fuel cells and electrolysis cells, and concentrated solar thermal power systems. Professor PL is an active member of the American Society of Mechanical Engineers. He is also a reviewer of papers for more than 10 technical journals.

JK received his M.S. degree (2007) from the Department of Aerospace and Mechanical Engineering at the University of Arizona in 2007. He is currently a Ph.D. student in the Department of Mechanical and Aerospace Engineering at the University of Texas at Arlington, USA. His research focuses on thermal/fluid sciences in energy system, modeling and system dynamics of solid oxide fuel cell and gas turbine (GT) hybrid systems. His Ph.D. dissertation work is the integrated modeling approach of solid oxide fuel cell-based combined heat and power (CHP) system.

HL received her bachelor degree (2005) in energy and power engineering area from Xi'an Jiaotong University, China. She is currently a Ph.D. student in the Department of Aerospace and Mechanical Engineering at the University of Arizona, USA. Her research focuses on numerical analysis of fluid flow and heat transfer in industrial processes and energy systems. Her Ph.D. dissertation work is experimental and numerical study of the multi-physics transport phenomena in internal reforming solid oxide fuel cells.

Received: 20 January 2012 Accepted: 27 April 2012
Published: 27 April 2012

References

1. Rowe, A, Li, X: Mathematical modeling of proton exchange membrane fuel cells. J. Power Sourc. **102**, 82–96 (2001)
2. Srinivasan, S, Mosdale, R, Stevens, P, Yang, C: Fuel cells: reaching the era of clear and efficient power generation in the twenty-first century. Annu. Rev. Energ. Environ. **24**, 281–328 (1999)
3. Gardner, FJ: Thermodynamic processes in solid oxide and other fuel cells. Proc. Inst. Mech. Engrs. **211**, 367–380 (1997)
4. Suzuki, K, Iwai, H, Kim, JH, Li, PW, Teshima, K: Solid oxide fuel cell and micro gas turbine hybrid cycle and related fluid flow and heat transfer. In: The 12th International Heat Transfer Conference, Grenoble France 18–23 August 2002
5. Roshandel, R, Arbabi, F, Karimi Moghaddam, G: Simulation of an innovative flow-field design based on a bio inspired pattern for PEM fuel cells. Renew. Energ. **41**, 86–95 (2012)
6. Ferng, YM, Su, A: A three-cell CFD model used to investigate the effects of different flow channel designs on PEMFC performance. Int. J. Hydrogen Energ. **32**, 4466–4476 (2007)
7. Yan, W-M, Yang, C-H, Soong, C-Y, Chen, F, Mei, S-C: Experimental studies on optimal operating conditions for different flow field designs of PEM fuel cells. J. Power. Sourc. **160**, 284–292 (2006)
8. Wang, X-D, Duan, Y-Y, Yan, W-M, Peng, X-F: Effects of flow channel geometry on cell performance for PEM fuel cells with parallel and interdigitated flow fields. Electrochim. Acta **53**, 5334–5343 (2008)
9. Manso, AP, Marzo, FF, Garmendia Mujika, M., Barranco, J., Lorenzo, A.: Numerical analysis of the influence of the channel cross-section aspect ratio on the performance of a PEM fuel cell with serpentine flow field design. Int. J. Hydrogen Energ. **36**, 6795–6808 (2011)
10. Lobato, J, Canizares, P, Rodrigo, MA, Pinar, JF, Mena, E, Ubeda, D: Three-dimensional model of a 50 cm^2 high temperature PEM fuel cell. Study of the flow channel geometry influence. Int. J. Hydrogen Energ. **35**, 5510–5520 (2010)
11. Li, P-W, Ki, JP: Analysis and optimization of current collecting systems in PEM fuel cells, Paper No. FUELCELL2007-25060. In: Proceedings of FUELCELL2007, Fifth International Conference of Fuel Cell Science, Engineering and Technology, New York, 18–20 June 2007
12. Goebel, SG: Impact of land width and channel span on fuel cell performance. J. Power Sourc. **196**, 7550–7554 (2011)
13. Hashemi, F, Rowshanzamir, S, Rezakazemi, M: CFD simulation of PEM fuel cell performance: effect of straight and serpentine flow fields. Math. Comput. Model. **55**, 1540–1557 (2012)
14. Peng, L, Lai, X, Liu, D, Hu, P, Ni, J: Flow channel shape optimum design for hydroformed metal bipolar plate in PEM fuel cell. J. Power Sourc. **178**, 223–230 (2008)
15. Yen, C-Y, Liao, S-H, Lin, Y-F, Hung, C-H, Lin, Y-Y, Ma, C-C: Preparation and properties of high performance nanocomposite bipolar plate for fuel cell. J. Power Sourc. **162**, 309–315 (2006)
16. Jayakumar, K, Pandiyan, S, Rajalakshmi, N, Dhathathreyan, KS: Cost-benefit analysis of commercial bipolar plates for PEMFC's. J. Power Sourc. **161**, 454–459 (2006)
17. Hontanon, E, Escudero, MJ, Bautista, C, Garcia-Ybarra, PL, Daza, L: Optimisation of flow-field in polymer electrolyte membrane fuel cells using

computational fluid dynamics techniques. J. Power Sourc. **86**, 363–368 (2000)
18. Li, PW, Chen, SP, Chyu, MK: Novel gas distributors and optimization for high power density in fuel cells. J. Power Sourc. **140**, 311–318 (2004)
19. Li, PW, Schaefer, L, Chyu, MK: Multiple processes in solid oxide fuel cells. In: Sunden B, Faghri M (eds.) Transport Phenomena in Fuel Cells, pp. 1–42. WIT Press, Boston (2005) 2005:1–42.
20. Shimpalee, S, Dutta, S: Numerical prediction of temperature distribution in PEM fuel cells. Numer. Heat Tran. **38**, 111–128 (2000)
21. Scherer, GG: Interfacial aspects in the development of polymer electrolyte fuel cells. Solid State Ionics **94**, 249–257 (1997)
22. Mishra, V, Yang, F, Pitchumani, R: Measurement and prediction of electrical contact resistance between gas diffusion layers and bipolar plate for applications to PEM fuel cells. ASME J. Fuel Cell Sci. Technol. **1**, 2–9 (2004)
23. Lee, WK, Ho, CH, Zee, JWV, Murthy, M: The effect of compression and gas diffusion layers on the performance of a PEM fuel cell. J. Power Sourc. **84**, 45–51 (1999)
24. Hental, PL, Lakeman, BJ, Mepsted, GO, Adcock, PL, Moore, JM: New material for polymer electrolyte membrane fuel cell current collectors. J. Power. Sourc. **80**, 235–241 (1999)

doi:10.1186/2251-6832-3-2
Cite this article as: Li *et al.*: Analysis and optimization of current collecting systems in PEM fuel cells. *International Journal of Energy and Environmental Engineering* 2012 **3**:2.